

# On the Mixing Flow Structure of a Turbulent Cross Jet

Byung Joon Rho\*, Je Ha Oh\*\* and Dae Ok Lee\*\*\*

(Received May 10, 1994)

An experimental study on the structure of a turbulent cross jet mixing flow is presented. Diffusion rates, two and three dimensional flow structures, mean velocities, turbulence intensities and turbulent shear stresses of the mixing flow were measured as varying the velocity ratio. Self-similar forms for the dimensionless mean velocity and turbulent shear stress profiles were found, particularly a semi-empirical curve for the turbulent shear stresses was obtained by correlating the measurement data resulting a remarkable agreement. It was found that the deviation gradient( $\alpha$ ) is linearly correlated with the velocity ratio( $R$ ), and the cross section of the mixing flow is an elliptic form.

**Key Words:** Reynolds Stress, Iso-Velocity Contour, Extrapolation Method, Similarity, Self-Preserving Region, Corss Flow

## Nomenclature

$b$	: Half width of jet	$v'$	: Turbulent component in the $Y_v$ direction
$b_{Yv}$	: Half width of mixing flow in the $Y$ -direction	$w'$	: Turbulent component in the $Z_v$ direction
C.P.	: Geometrical cross point	$X$	: Axial direction
$D_0$	: Nozzle diameter	$X_0$	: Distance between the nozzle exit and C. P.
$R$	: Velocity ratio	$X_v$	: Axial direction of mixing flow( $R \neq 1.0$ )
$r$	: Radial distance	$Y$	: Radial direction
$\bar{U}$	: Axial mean velocity	$Y_v$	: Deviation distance between $X$ and $X_v$ axes
$\bar{U}_1$	: Exit mean velocity(lower side)	$Y_0$	: Half distance between nozzles
$\bar{U}_m$	: Axial maximum mean velocity	$Y_v$	: Radial direction of mixing flow( $R \neq 1.0$ )
$\bar{U}_0$	: Exit mean velocity(higher side)	$Z$	: Normal direction of $X$ - $Y$ plane
$u'$	: Turbulent component in the $X_v$ direction	$\alpha$	: Deviation gradient
$\overline{u'v'}$	: Reynolds' stress in the $X$ - $Y$ plane	$\eta$	: Defined as $Y/b$ or $Z/b$
$\overline{(u'v')_m}$	: Maximum Reynolds' stress in the $X$ - $Y$ plane	$\theta$	: Cross angle
$\overline{u'w'}$	: Reynolds' stress in the $X$ - $Z$ plane		
$\bar{V}$	: Radial mean velocity		

## 1. Introduction

This study was carried out to investigate the structure of a cross jet with velocity ratio variations. The turbulent mixing flow of the cross jet was created by two round jets issuing from circular nozzles with the same dimensions.

These kinds of complex cross jet flows develop in most combustion systems of various models such as a wall jet, a radial jet, an impinging jet,

\* Department of Precision Mechanical Engineering, Chonbuk National University, Chonju 560-756, Korea

\*\* Department of Precision Mechanical Engineering, Chonbuk National University, Chonju 560-756, Korea

\*\*\* Agency for Defense Development, Daejeon 305-600, Korea

etc.... The majority of mixing flows in the combustor are two phase turbulent mixtures of air and fuel, and the mixing conditions strongly affect the combustion. The turbulent mixing with or without swirl is expected to be governed by the mechanism of the jet system in the combustors.

Many papers have reported on the characteristic results obtained depending upon the different jet configurations respectively.

Andreopoulos(1982) presented the measurements of velocity fluctuation statistics in the jet-pipe of a jet in a cross-flow situation for various values of the jet-pipe to cross-flow velocity ratio. And he(Andreopoulos, 1985; Andreopoulos and Rodi, 1984) extended his study to obtain the results of spectral analysis and flow visualization for various ratios and Reynolds numbers of a jet issuing perpendicularly from a developing pipe flow into a cross flow. Results were reported of experiments by Kamotani and Grever(1972) on turbulent circular jets issuing into a cross flow, both for unheated and heated jets. Laser-Doppler measurements in a subsonic jet injected into a subsonic cross flow were made by Rudinger and Moon(1976).

Gencay, Tapucu et al.(1984) have experimentally investigated the diversion cross flow caused by subchannel blockages with different mass flow rates. Bojic and Eskinazi(1979) studied a two-dimensional and mathematical model of a non-buoyant jet in a cross flow and they calculated the mean velocity distribution for the mixing of a turbulent, nonbuoyant, round jet in a cross wind.

An investigation of the numerical prediction of the trajectories of turbulent triple jets issuing into a uniform cross flow was carried out by Makihata and Miyai(1983), and the diffusion of jets in a cross flow was studied by Shirakashi and Tomita(1978). Issac and Jakubowski(1985) have experimentally investigated the interaction of twin jets with a cross flow with the velocity ratio of 2.

Abramovich(1963) gave a detailed description of the processes of a turbulent jet in a cross flow. He observed that the cross section deformed into a horseshoe shape that could be similar to an ellipse.

In relation with these cross flows Rho, Kim, Park et al.(1984, 1985, 1986, 1987, 1989, 1990, 1991) have conducted experimental studies of a turbulent cross jet and intensively analyzed the turbulent mixing characteristics such as mean and fluctuating velocities, probability density distributions, intermittency factors, Reynolds stresses, etc. .... They found that the mixing flow configuration of half widths after crossing point formed an elliptic circle. This feature typically appeared in a certain limited area and deformed into a normal circular form in the far downstream in which the mixing flow might be sufficiently developed. The maximum mean velocity on the centerline showed an abrupt increase before the crossing point and decreased along the axial direction and non-dimensional mean velocity deficit profiles had a good similarity and could be formulated as a semi-empirical equation.

Ahmed and So(1987) have conducted an experimental study to investigate the characteristics of air jets discharging normally into a swirling cross-flow with the swirl ratios of 0.43 and 0.96. Kadota and Wang(1990) examined the structure of a propane jet diffusion flame discharged normal to a free stream of air with a uniform velocity profile by LDV system. And recently multiple turbulent jets through a cross flow have attracted much interest and Barata et al.(1991, 1992) have performed multiple impinging jets in a cross flow and intensively analyzed the mean and turbulent velocity characteristics of the flow field, and the results were compared with the visualizations. In some different way, an experimental study on the mixing of one-and dual line heated jets with a cold crossflow in a confined channel was carried out by Chen and Hwang(1991), and the results of mean temperature, velocity and turbulence intensity with flow visualizations were presented.

Savory(1991) and Toy(1982) examined the interaction between twin side-by-side circular jets issuing into a crossflow by taking advantage of a video system, and their recent study(Toy et al., 1993) is focused on the turbulent mixing flow characteristics depending upon the cross angle and they fixed it as 30 and 45 degrees as conducted by Rho et al.

In this study, the measurements of turbulence components were made by a two channel hot-wire anemometry connected to an on-line data acquisition computer system and the electric micro-manometers were utilized to check the stability of the flow and calibrate the system.

As the experimental results, the turbulent mixing flow structures such as cross sections, two-dimensional flow fields, three-dimensional flow structures have been intensively investigated, and the mean and fluctuating components, Reynolds' stresses were analytically discussed.

## 2. Experimental Set-Up

An open type subsonic wind tunnel with a contraction ratio of 9:1 was utilized as a main flow generating system. In order to stabilize and diminish the turbulent fluctuations of the flow two honey-combs and three grids were set up in the settling chamber. The original flow has been generated by a centrifugal type blower coupled with V.S. motor of 3 phase 220 V, 3.75 KW, and the flow velocity could be available. The flow in the test section ( $200 \times 200 \times 400 \text{ mm}^3$ ) was proved to be stable and had uniform distributions, and the intensity of turbulence was negligibly small (below 0.1%).

A cross jet equipment was designed to have two circular contraction nozzles with the same dimensions as illustrated in Fig. 1. This equipment consists of two straight inlet pipes of 50 mm in diameter and 175 mm long, two flow guide tubes which are smoothly curved to make a cross angle of 45 degrees and two contraction circular noz-

zles. The two nozzles were set up at the end of the guide tubes and made a angle of  $\theta = 45$  degrees each other. In consequence, the jet flow issuing from a nozzle was oriented towards the X-direction with a angle of 22.5 degrees as shown in the figure. The details of the nozzles are given in Fig. 1. In order to control even a minimum difference of dynamic pressure that might occur at the exits of the nozzles, a ball valve was utilized by setting it in the straight inlet pipe. Two grids were inserted after the ball valve to stabilize the flow.

As a data acquisition system, a two channel hot-wire anemometer set (Tsi, 1050 series) connected to an on-line computer analyzing work station has been utilized. X-type hot-wires of  $5 \mu\text{m}$  in diameter and 2 mm in length, made of tungsten (Tsi model T5) were used as a probe, and the displacement of the probes has been controlled by an automatic probe traversing unit (FCO60) with a precision of 0.1 mm. The moving distances and time intervals were controlled by a micro processor unit.

## 3. Measurement Techniques

A mixing flow configuration of a turbulent cross jet developed by two round jets could be predicted as shown in Fig. 2. Since this type of cross jet has many experimental parameters such as a cross angle, distance between two nozzles, velocity ratio, number of nozzles etc..., the measurements should be made under some fixed conditions. And in this study the distance between two nozzles was fixed as 180 mm, the

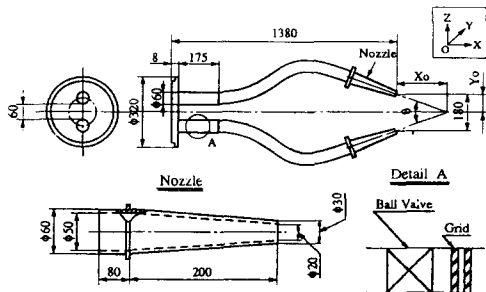


Fig. 1 Geometry of a cross jet kit

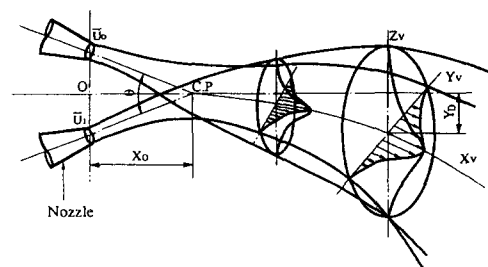


Fig. 2 Flow configuration of a cross jet ( $R \neq 1.0$ )

cross angle as 45 degrees and the two circular contraction nozzles have the same dimensions, and only the velocity ratio has been taken as an experimental parameter. The exit velocities issuing from each nozzle were precisely manipulated with the ball valve to have the velocity ratios of 1.0, 0.8, 0.6, 0.4.

The data have been measured in the region of  $1 \leq X/X_0 \leq 2.5$  which experimentally proved to be an intensive turbulence developing region (Rho. and Kim., 1984) and on which much interest is concentrated since most of the turbulent mixing flows immediately after the impingement govern the combustion processes in the combustors.

The probe displacements were conducted in the  $Y(Y_v)$  and  $Z$  axes at each axial position of  $X(X_v)$ , and these measurements have been repeated for each velocity ratio. During the measurements the exit velocities were systematically checked by an electric micro-manometer with a precision of a 0.1 mm water column to keep a constant ratio.

Statistical method was adapted for data samplings by an on-line computer measurement system consisting of a two channel hot-wire set, 32 bit computer with a special assistant board supported by a S/W(GASPIN). This system made it possible to treat the ensemble data in 5 seconds for samplings of mean and fluctuating velocities, Reynolds stress, flatness and skewness factors, one and joint probability densities, correlation coefficients etc....

To minimize the errors that might occur in measurements, the data at each position have been sampled up to 40000 for taking a mean value. And the data has been continuously checked by repeating the measurement for high reliability.

## 4. Results and Discussions

### 4.1 Diffusion and cross sections

In general, when the two round jets with the same geometrical dimensions and Reynolds numbers combine together in parallel or cross jets, the maximum velocity path line of the mixing flow does not deviate from the central axis. But the

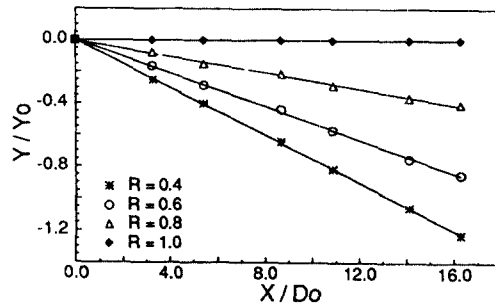


Fig. 3 Centerlines of a mixing flow

center line of the mixing flow for  $R=1.0$  deviates from the original axis for  $R=1.0$  and the deviation increases with the decrease of velocity ratio  $R$ . As shown in Fig. 3 the deviation rates are distinctly different in accordance with the velocity ratios, but the deviation gradients in the downstream direction are linearly correlated in the range of  $X/D_0 \leq 16.0$ . The data presented in the figure are the positions of maximum velocities measured on the  $X$ - $Y$  central plane along the axial direction.

Figure 4 illustrates the relation between the deviation gradients( $\alpha$ ) and the velocity ratios( $R$ ), and the correlation is empirically given for the case of  $\theta=45$  degrees,

$$\alpha = 0.122 R - 0.122 \quad (1)$$

and then the path line of the maximum velocities for each velocity ratio can be expressed as

$$Y/Y_0 = (0.122 R - 0.122)(X/D_0). \quad (2)$$

Abramovich(1963) has given a detailed description of the processes involved in the diffraction of

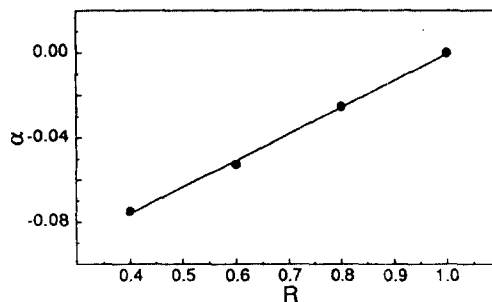


Fig. 4 Correlation between the deviation gradient( $\alpha$ ) and the velocity ratio( $R$ )

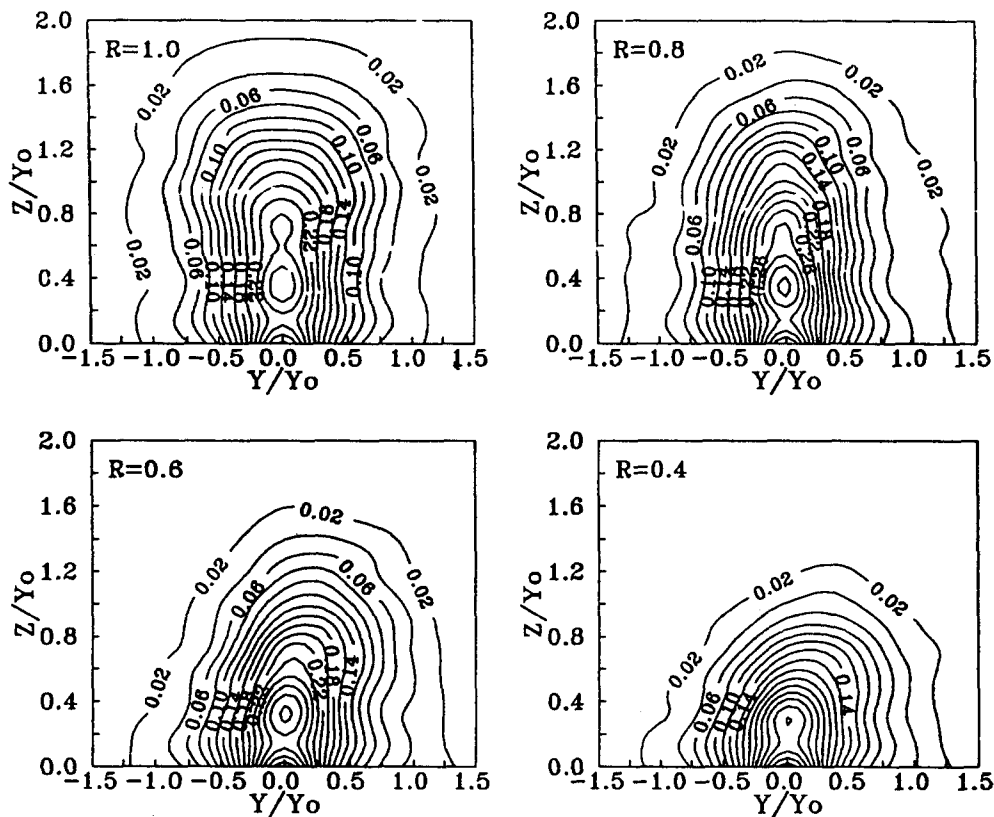


Fig. 5 Structures of the mixing flow cross section measured at  $X/X_0=1.8$

a turbulent cross jet. He observed that the mixing flow cross section formed an elliptic shape. This observation has been also conducted by Rho et al. (1984, 1990). They formulated a semi-empirical elliptic equation by taking advantage of the experimental data. However the elliptic shape deformed into a circular one and the empirical equation was not available in the far downstream.

Figure 5 denotes the mixing flow cross section measured at  $X/X_0=1.8$  depending upon the velocity ratio for the cross angle of 45 degrees. Each line represents the iso-velocity contour and the cross section shows an elliptic shape which is differently formed depending on the velocity ratio.

These cross sections of the mixing structures formed an unusual elliptic shape since the mixing flows are in the developing process and the

measurements were made relatively near to the cross point. By virtue of the different momentum fluxes of two jets, the top-viewed central cross sections are bended like a banana towards the low velocity side. This phenomenon can be more distinctly observed in lower velocity ratios.

The  $Y$ -directional widths of the cross section are comparatively consistent except for  $R=1.0$  while  $z$ -directional ones show a gradual decrease with the lower velocity ratio. And the velocity ratio seems to be a parameter strongly affecting diffusions in the  $Z$ -direction.  $Y$ -directional diffusion flows are expected to be rather contracted near the cross point and the diffusion rate grows slowly compared to a single free jet. As the decrease of velocity ratio means the decrease of the total mixing flow rates, the cross-sectional area of the mixing flow becomes smaller.

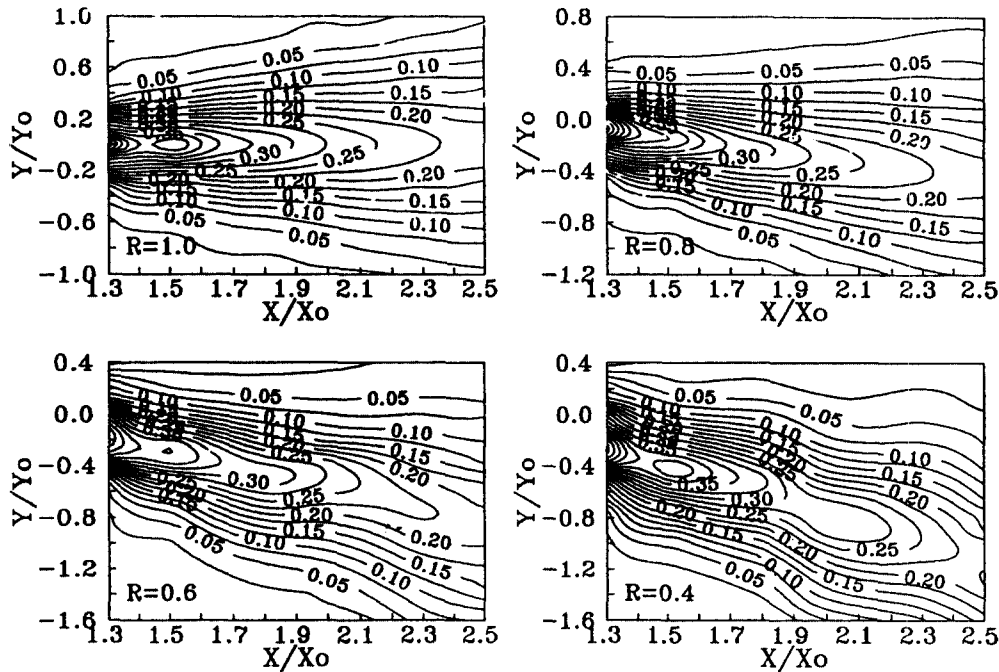


Fig. 6 Two-dimensional structures of a mixing flow field

#### 4.2 Two-dimensional flow fields

Iso-contours of two-dimensional velocity distributions in the central  $X$ - $Y$  plane are presented in Fig. 6. The resultant velocity values have been calculated from  $\bar{U}$  and  $\bar{V}$  for the analyses of actual flow directions, and an extrapolation method was employed to obtain the continuous contours between the neighboring measuring positions in which the same level mean velocities were measured. The two-dimensional structures illustrate axisymmetric distributions on the  $X$ - $Y$  planes, in particular, the contours for  $R=1.0$  show complete similarities to a single round jet. As shown in figures for  $R=0.8, 0.6, 0.4$ , the mixing flow directions are found to be fixed immediately after the cross point and the diffusion rates on both sides about the maximum velocity locations are similarly distributed. Since the centerlines of the original jets were aligned to exist on a horizontal  $X$ - $Y$  plane, the mixing flows might be contracted and unusual diffusing flows occurred on  $Y(Y_0)$  axis in the confined regions of undeveloped mixing flow.

#### 4.3 Three-dimensional flow structures

Visualization methods are sometimes actually utilized to investigate the structures and characteristics of the flow, however, in air jets with high Reynolds numbers to obtain an expected result is almost impossible particularly in the mixing flow of a turbulent cross jet any visible structures are not apt to be visualized. In the strongly developed turbulent mixing flow, there have been many difficulties in measurement of the exact outer boundaries of the flow due to the irregular fluctuations. Then, in this study to observe the schematic configurations of the streamwise mean flows, the positions of half maximum velocities were measured and illustrated in Fig. 7.

As the flows are mixed by different jets with high turbulent intensity levels, the three-dimensional structures are irregularly deformed and an axisymmetric configuration can not be observed. This phenomenon more significantly appeared in the lower velocity ratios since the strong perturbations are usually produced in the mixing process between two different jets and

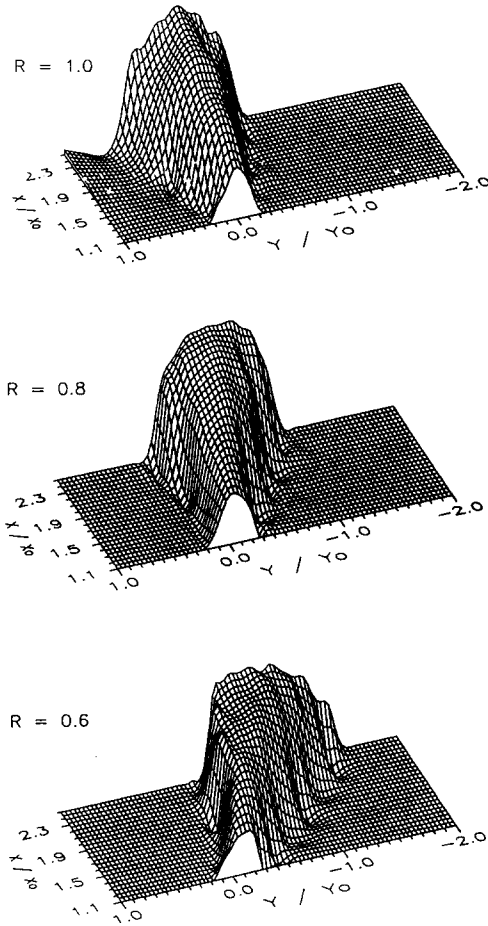


Fig. 7 Three-dimensional structures of a mixing flow field

even more in the cross jets.

#### 4.4 Mean velocity distributions

The turbulent mixing flow discussed in this experiment is quite complex in order to analyze its exact structures and characteristics, since the original jets used to create the mixing flow have different Reynolds numbers and collide at 45 degrees with respect to each other. Therefore the mixing flow actually begins after the cross point and the fully-developed mixing structure can be expected in the far downstream. Once two round jets combine together by colliding at 45 degrees, they become a flattened free jet, and it changes

into an elliptic form and finally a circular one in the self-preserving flow region.

Most of the turbulent equations have been derived by considering the flow conditions in the fully-developed region.

Hinze(1975) and Tollmien(1963) derived semi-empirical formulae for a turbulent jet by taking advantage of the theoretical turbulent equations which were simplified by omitting several terms in the Reynolds' ones under the characterized flow boundary conditions. Consequently, with some modifications, they introduced their experimental constants and suggested the semi-empirical equations as follows

Hinze :

$$\frac{\bar{U}}{U_m} = (1 + 0.414 \eta^2)^{-2} \quad (3)$$

Tollmien :

$$\begin{aligned} \frac{\bar{U}}{U} = & \{1 - 0.202(1.225 \eta)^{1.5} \\ & - 0.00204(1.225 \eta)^3 \\ & + 0.041(1.225 \eta)^{4.5} + \dots\} \\ & \times \exp\{-0.26937(1.225 \eta)^{1.5} \\ & - 0.00136(1.225 \eta)^3 \\ & + 0.00018(1.225 \eta)^{4.5} + \dots\}. \quad (4) \end{aligned}$$

While a similar equation for a plane jet was given by Görtler and Schlichting's formula was discussed in the wake flow. An another equation for axisymmetric flows was formulated by Gauss and used very often for comparisons of mean velocity distributions.

$$\text{Görtler : } \frac{\bar{U}}{U_m} = 1 - \tanh^2(0.881 \eta) \quad (5)$$

$$\text{Schlichting : } \frac{\bar{U}}{U} = \{1 - (0.414 \eta)^{1.5}\}^2 \quad (6)$$

$$\text{Gauss : } \frac{\bar{U}}{U_m} = \exp(-0.693 \eta^2). \quad (7)$$

Wynanski and Fiedler(1969) suggested in their circular jet that the fully-developed turbulent region could be expected farther than  $40 d$  in the downstream direction. In the mean time Townsend(1976) described that the self-preserving flow region could be observed near  $50 d$  apart from the nozzle exit. Hence, in most of the turbulent jets the self-preserving flow region is usually discussed in the far downstream( $X \geq 40$

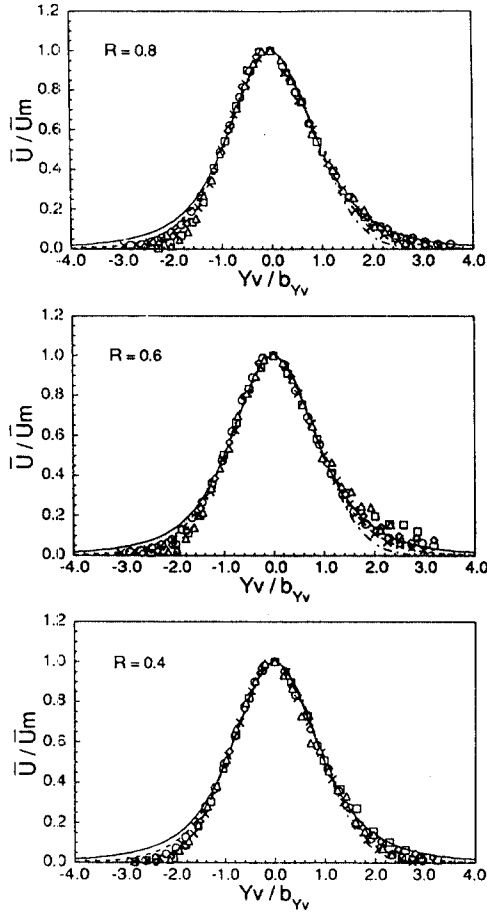


**Fig. 8** Axial mean velocity distributions of a mixing flow  
 ( $\times$  :  $X_v/X_0=1.3$ ,  $\circ$  :  $X_v/X_0=1.5$ ,  $\diamond$  :  $X_v/X_0=1.8$ ,  $\square$  :  $X_v/X_0=2.0$ ,  $\triangle$  :  $X_v/X_0=2.5$ , — : Hinze,  $\cdots$  : Görtler, - - - : Gauss)

d). The equations referenced above are not available for this kind of complex cross jets since the mixing regions interested in this experiment are not yet sufficiently developed to be considered as a self-preserving flow region. However some of these equations have been employed for the global comparisons with the data obtained.

Figure 8 denotes the axial mean velocity distributions measured in the mixing flow regions ( $1.1 \leq X_v/X_0 \leq 2.5$ ) depending upon the velocity ratios. Though the data acquisitions were made in the undeveloped region, remarkable similarities could be observed mostly in the half width sections independent of axial positions and velocity

ratios. The semi-empirical curves of Hinze, Görtler and Gauss show an agreement only in the half width sections but not in outer regions because the equations were modified under the different conditions in simplifying the terms and introducing the experimental constants. As the two jets collide at 45 degrees, the mixing flow after the cross point comes to be contracted on the  $Y(Y_v)$  axis and begins to develop a diffusing flow. Therefore the axial mean velocity distributions on the  $Y(Y_v)$  axis show a relatively good similarity compared with those on the  $Z(Z_v)$  axis, while an abrupt expanding flow occurs in the  $Z(Z_v)$  direction by virtue of colliding forces and any good similarity can hardly be observed in the undeveloped mixing flow regions.

As shown in the figures, the experimental data and the semi-empirical curves have a good agreement in the half width core region, while some scatterances occurred in the outer regions. Through these three figures, the data on the right side (higher jet side) show higher values than the left side (lower jet side).

The highest scatterance in the outer flow regions was found in the figure of  $R=0.6$  and it appeared distinctly on the higher jet side. And the velocity distribution profiles of  $R=0.6$  showed the most unbalanced pattern among three velocity ratios, but this unbalanced distributions are found to be remarkably equilibrated for  $R=0.4$  as for  $R=0.8$ . This fact can be predicted that the higher jet governs the mixing flow with larger mass flow rates immediate after collision.

#### 4.5 Intensities of turbulence

Three dimensional fluctuating components measured on the  $X_v$  axis are presented in Fig.9. The higher levels of intensity of turbulence for all components are observed in the range of  $1.5 \leq X_v/X_0 \leq 2.0$  independent of mass ratios, and the maximum values are found in the near region of  $X_v/X_0 \approx 1.8$ . The intensity levels of three components do not have remarkable differences among their corresponding components depending upon the velocity ratio respectively.

It is generally known that the turbulent levels of  $v'$  and  $w'$  components in a turbulent round jet



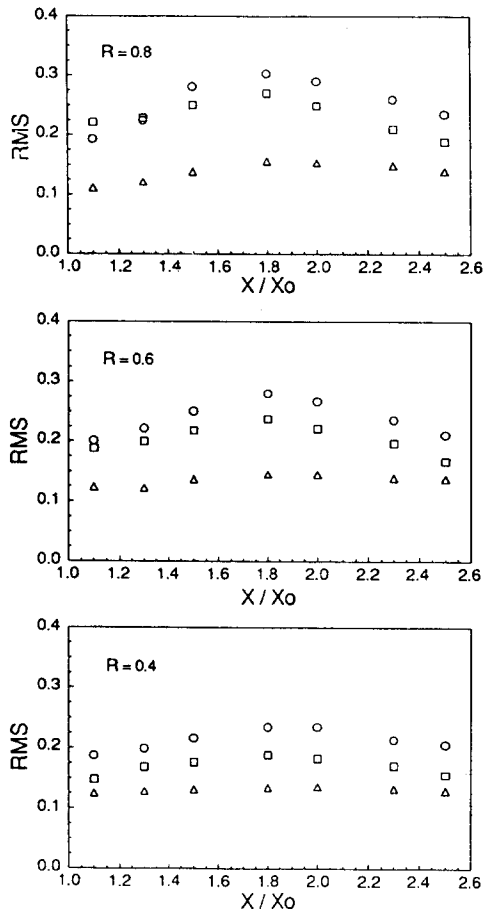


Fig. 9 Distributions of intensity of turbulence (○:  $\overline{u'}/\overline{U_{ct}}$ , □:  $\overline{v'}/\overline{U_{ct}}$ , △:  $\overline{w'}/\overline{U_{ct}}$ )

used to be of the same order, but these estimations can not be expected in this experiment as illustrated in the figure.

The developments of the  $w'$  component for all mass ratios are found to be much smaller than those of  $u'$  and  $v'$  as the combined mixing jet develops and diffuses differently in the  $Y(Y_v)$  and  $Z(Z_v)$  directions. However, these differences of intensity levels become gradually smaller with the decrease of velocity ratio. This feature is distinctly observed in case of  $R=0.4$ .

4.6 Turbulent shear stresses

In a simple round or plane jet, the mean velocity components and turbulent shear stresses are axisymmetrically distributed. But in this kind of

complex cross jet turbulent shear stresses are scattered and have asymmetric values.

Görtler has suggested an adaptable equation of turbulent shear stresses for a plane jet and gave the form,

$$\frac{\overline{u'v'}}{u^2} = \frac{1}{2} \frac{db}{dx} f(\eta) \int_0^\eta f(\eta) d\eta \quad (8)$$

and Hinze gave a similar description for a round jet,

$$\frac{\overline{u'v'}}{u^2} = \frac{1}{2} \frac{db}{dx} \frac{f(\eta)}{\eta} \int_0^\eta \eta f(\eta) d\eta. \quad (9)$$

These two expressions do not have a good similarity with the experimental random data. Then Elliott and Townsend(1981) suggested a semi-empirical form obtained from the experimental data in a turbulent wake flow in a distorting duct.

$$\frac{|\overline{u'w'}|}{|\overline{u'w'_m}|} = e^{\frac{1}{2} \frac{z}{l_0}} \exp\{-\frac{1}{2}(z/l_0)^2\} \quad (10)$$

where  $l_0$  is the width scale defined as  $l_0^2 = \int (u_1 - u)^2 z^2 dz / \int (u_1 - u) dz$  and  $u_1$  is the mean velocity value in the absence of a cylinder in the flow. Similarly, Rho et al.(1987) have also derived an agreeable semi-empirical equation in a turbulent cross jet.

$$\frac{|\overline{u'v'_r}|}{|\overline{u'v'_r}_m|} = 2.787(r/b) \exp\{-1.4286(r/b)^2\}. \quad (11)$$

These four equations mentioned above have different original conditions respectively and the Eq. (11) was obtained from the data treated in the mixing flows of non self-preserving regions. There

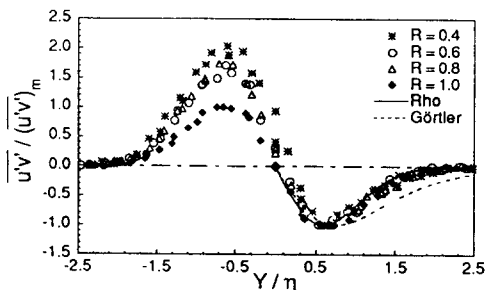


Fig. 10 Distributions of the turbulent shear stresses in the  $X$ - $Y$  plane at  $X/X_0=1.8$  and 2.5

appeared some scatterances and deviations among the curves.

The data obtained in these measurements for  $X/X_0=1.8, 2.5$  are illustrated in Fig. 10. As the two turbulent jets combined into a mixing flow the turbulent shear stresses show remarkably different values on both sides of the  $Y_v$  axis.

The experimental data has been normalized by the maximum value of  $\overline{u'v'}$  measured on the lower jet side to compare the distributions and the order of magnitudes. As illustrated in the figure, the maximum values on the higher jet side for  $R \leq 0.8$  are evaluated as much as 1.5~2.0 times of the lower jet side. The theoretical equation of Görtler and the semi-empirical one suggested by Rho are presented with the experimental data. As was expected, the order of magnitudes on both sides of the  $Y(Y_v)$  axis does not show the same level. The distribution curve for  $R=1.0$  is presented as a perfect axisymmetry, while the other curves for  $R \neq 1.0$  are shown as asymmetric patterns. While the Rho's empirical curve agrees well with the data, on the other hand, Görtler's theoretical curve deviates apparently from the experimental results. These characteristics shall be reasonably accepted since the correlation equations were derived under different flow conditions.

The data measured on both sides of the  $Y(Y_v)$  axis is presented in Fig. 11. The measurements have been made in the regions of  $X/X_0=1.8, 2.5$  for  $R=1.0, 0.8, 0.6, 0.4$ , and the data was normalized by the maximum value for each side respectively. As shown in the figure, most of the data is concentrated on the solid curve and the maximum

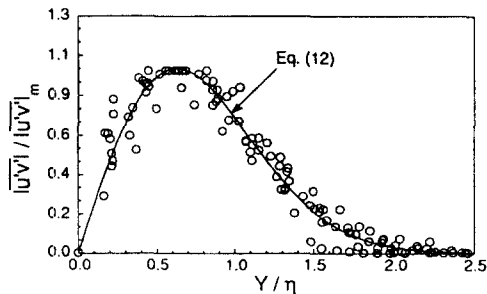


Fig. 11 Distributions of the turbulent shear stresses in the  $X$ - $Y$  plane

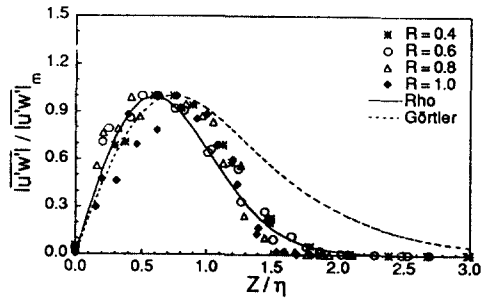


Fig. 12 Distributions of the turbulent shear stresses in the  $X$ - $Z$  plane at  $X/X_0=1.8$  and  $2.5$

values are found in the regions of  $0.5 \leq Y(Y_0)/h \leq 0.7$ . The curve plotted in the figure was correlated as follows and gives approximately a 1.8% error.

$$\frac{|u'v'|}{|u'v'|_m} = 2.658(Y_0/\eta) \exp[-1.268(Y_0/\eta)^2]. \quad (12)$$

As the combined jet diffuses typically in the  $Z(Z_v)$  direction, the mean and turbulent structures may show similar patterns on both sides about the axis. The data presented in Fig. 12 has been measured on the  $Z(Z_v)$  axis for  $R=1.0, 0.8, 0.6, 0.4$  in the regions of  $X/X_0=1.8, 2.5$ . The theoretical curve of Görtler and Rho's semi-empirical curve are compared with the present data. This figure denotes that the Görtler's curve deviates remarkably from the experimental data while Rho's curve shows a relatively good agreement.

This result as discussed above, may be caused by the original conditions considered in the derivation processes of the equations. It may be naturally accepted that the data does not exhibit a complete concentration on a curve, since the strong colliding forces and an abrupt expanding flow affect the turbulent structures and govern strongly the development of turbulent components.

## 5. Conclusions

For the experimental investigations performed in a certain limited mixing flow regions, some concluding remarks can be summarized as follows;

The path line of the mixed maximum velocity

has a linear relationship between the deviation gradients( $\alpha$ ) and velocity ratios( $R$ ).

The cross sectional structures deform with the mass ratio and this "banana shaped" deformation is more apparent with lower mass ratios.

Two-dimensional flow fields, illustrated with iso-contours of resultant velocities, show a remarkable axisymmetric distributions about the mixed flow axis independent of velocity ratios. The flow fields bended toward the lower velocity side and the orientation of a mixing flow was observed to be fixed immediate after collision.

Three-dimensional configurations obtained from experimental data were found to be a reliable way the visualize invisible fluid flows with high velocity.

The non-dimensional axial mean velocity profiles have a good agreement with the previous semi-empirical curves and showed complete similarities in the central regions independent of mass ratios. While some scatterances of the data were observed and a different order of values in the outer boundary layers developed due to the different jet velocities.

The intensities of turbulence is developed strongly in the region of  $X/X_0 \approx 1.8$  and showed its highest value at this position. The RMS values of  $u'$ -components were twice or more as much as those of  $w'$ -components.

The Reynolds stresses of  $\overline{u'v'}$  were asymmetrically distributed about the axis of the mixing flow in the  $X$ - $Y$  plane but the data, normalized by each maximum Reynolds stress, was found to be concentrated on an exponential empirical curve, and the distributions of  $\overline{u'w'}$  showed a similar pattern.

## References

- Abramovich, G. N., 1963, "The Theory of Turbulent Jets," MIT Press, Cambridge, MA, pp. 541~553.
- Ahmed, S. A. and So, M. C., 1987, "Characteristics of Air Jets Discharging Normally into a Swirling Crossflow," *AIAA Journal*, Vol. 23, No. 3, pp. 429~435.
- Andreopoulos, J. and Rodi, W., 1984, "Experimental Investigation of Jets in a Crossflow," *J. of Fluid Mech.*, Vol. 138, pp. 93~127.
- Andreopoulos, J., 1982, "Measurement in a Jet-Pipe Flow Issuing Perpendicularly into Cross Stream," *ASME, J. of Fluids Engineering*, Vol. 104, pp. 493~499.
- Andreopoulos, J., 1985, "On the Structure of Jets in a Crossflow," *J. of Fluid Mech.* Vol. 157, pp. 163~197
- Barata, J. M. M., Durao, D. F. G. and Heiter, N. V., 1992, "Velocity Characteristics of Multiple Impinging Jets Through a Crossflow," *ASME Journal of Fluids Engineering*, Vol. 114, pp. 231~239.
- Barata, J. M. M., Durao, D. F. G. and Heitor, M. V., 1991, "Impingement of Single and Twin Turbulent Jets Through a Crossflow," *AIAA Journal*, Vol. 29, No. 4, pp. 595~602.
- Bojic, M. L. and Eskinazi, S., 1979, "Two-Dimensional Mathematical Model of a Non-buoyant Jet in a Crossflow," *AIAA Journal*, Vol. 17, No. 10, pp. 1050~1054.
- Chen, K. S. and Hwang, J. V., 1991, "Experimental Study on the Mixing of One-and Dual-Line Heated Jets with a Cold Crossflow in a Confined Channel," *AIAA Journal*, Vol. 29, No. 3, pp. 353~360.
- Elliott, C. and Townsend, A. A., 1981, "The Development of a Turbulent Wake in a Distorting Duct," *J. of Fluid Mech.*, Vol. 113, pp. 433~467.
- Gencay, S., Tapucu, A., Troche, N. and Merilo, M., 1984, "Experimental Study of the Diversion Crossflow Caused by Subchannel Blockages, Part I : Experimental Procedures and Mass Flow Rates in the Channels," *ASME J. of Fluids Engineering*, Vol. 106, pp. 435~440.
- Hinze, J. O., 1975, *Turbulence*, 2nd Ed., McGraw-Hill.
- Isaac, K. M. and Jakubowski, A. K., 1985, "Experimental Study of the Interaction of Multifluid Jets with a Cross Flow," *AIAA Journal*, Vol. 23, No. 11, pp. 1679~1683.
- Kadota, T. and Wang, J. X., 1990, "Structure of Propane Jet Diffusion Flame in a Cross Flow," *JSME International Journal, Series II*, Vol. 33, No. 3, pp. 575~581.

- Kamotani, Y. and Greber, I., 1972, "Experiments on a Turbulent Jet in a Cross Flow," *AIAA Journal*, Vol. 10, No. 11, pp. 1425~1429.
- Makihata, T. and Miyai, Y., 1983, "Prediction of the Trajectory of Triple Jets in a Uniform Crossflow," *ASME J. of Fluids Engineering*, Vol. 105, pp. 91~97
- Rho, B. J. and Kim, J. K., 1987, "A Comparative Study on the Round Jet and the Cross Jet," *KSASS*, Vol. 15, No. 1, pp. 23~34.
- Rho, B. J. and Kim, J. K., 1984, "An Experimental Study on the Turbulent Flow of a Free Cross Jet," *KSME*, Vol. 8, No. 5, pp. 442~449.
- Rho, B. J. and Kim, J. K., 1986, "Study on the Statistical Turbulent Characteristics of 45° Circular Cross Jet Flow," *KSME*, Vol. 10, No. 1, pp. 110~120.
- Rho, B. J. and Park, J. H., 1988, "Study on the Statistical Turbulence Characteristics of Cross Jets in the Cylinder by On-Line Computer System," *KSME*, Vol. 12, No. 4, pp. 876~891.
- Rho, B. J., Kim, J. K. and Dwyer, H. A., 1990, "Experimental Study of a Turbulent Cross Jet," *AIAA Journal*, Vol. 28, No. 5, pp. 784~789.
- Rho, B. J., Lee, D. O., Kim, J. S. and Oh, J. H., 1991, "Topological and Statistical Investigation of a Cross Jet Formed by Two Different Jets," *KSME*, Vol. 15, No. 4, pp. 1301~1308.
- Rudinger, Y. and Moon, L. F., 1976, "Laser-Doppler Measurement in a Subsonic Jet Injected into a Subsonic Crossflow," *ASME J. of Fluids Engineering*, Vol. 98, No. 3, pp. 515~520.
- Savory, E. and Toy, N., 1991, "Real-Time Video Analysis of Twin Jets in a Crossflow," *ASME*, Vol. 113, pp. 68~72.
- Schlichting, H., 1979, *Boundary Layer Theory*, 7th Ed., McGraw-Hill.
- Shirakashi, M. and Tomita, Y., 1978, "The Diffusion of Jets in a Cross Flows," *Bulletin of the JSME*, Vol. 21, No. 157, pp. 1160~1167.
- Tapucu, A., Gencay, S., Troche, N. and Merilo, M., 1984, "Experimental Study of the Diversion Crossflow Caused by Subchannel Blockages, Part II : Pressures in the Channels and the Comparison of the COBRA III-C Predictions With Experimental Data," *ASME J. of Fluids Engineering*, Vol. 106, pp. 441~447
- Townsend, A. A., 1976, *The Structure of turbulent Shear Flow*, 2nd Ed., Cambridge University Press.
- Toy, N., Disimile, P. J., Savory, F. and McCusker, S., 1992, "The Development of the Interface Region Between Twin Circular Jets and a Normal Crossflow," *Proceedings, 13th Symposium on Turbulence*, Rolla, U.S.A.
- Toy, N., Savory, E., Shoe, B. and Disimile, P. J., 1993, "Digital Image Analysis of Two Impinging Circular Jets," *Engineering Turbulence Modelling and Experiments 2*, Elsevier Ed., pp. 425~434.
- Wynanski, I. and Fiedler, H., 1969, "Some Measurements in the Self-Preserving Jets," *J. of Fluid Mech.*, Vol. 38, part 3, pp. 577~612.